Drug Design, Development and Therapy

Dovepress

open access to scientific and medical research

Open Access Full Text Article

ORIGINAL RESEARCH

Aloin Inhibits the Proliferation and Migration of Gastric Cancer Cells by Regulating NOX2–ROS-Mediated Pro-Survival Signal Pathways

This article was published in the following Dove Press journal:
Drug Design, Development and Therapy

Ziqian Wang[1,2]
Tuo Tang[1,2]
Shengnan Wang[1,2]
Tianyu Cai[1,2]
Hong Tao[1,2]
Qing Zhang[1,2]
Shimei Qi[1,2]
Zhilin Qi[1,2]

[1]Department of Biochemistry and Molecular Biology, Wannan Medical College, Wuhu, Anhui 241002, People's Republic of China; [2]Anhui Province Key Laboratory of Active Biological Macro-Molecules, Wannan Medical College, Wuhu, Anhui 241002, People's Republic of China

Background: Aloin has been reported to have many pharmacological effects including anti-inflammatory, anti-oxidant and anti-tumour activities. However, the precise molecular mechanisms underlying the anti-tumour properties of aloin are yet to be elucidated.

Methods: HGC-27 and BGC-823 gastric cancer cells were treated with aloin. EdU and colony formation assays were used to detect the proliferation ability of cells. The migration of cells was detected using wound healing and transwell assays. Western blotting was used to detect the levels of cyclinD1, cyclin E1, MMPs, N-cadherin, E-cadherin and NOX2. The phosphorylation of Akt, mTOR, P70S6K, S6, Src, stat3 and IκBα were also detected by Western blotting. Flow cytometry was used to detect the cell cycle distribution.The location of p65 in cells was determined by using a confocal microscopy assay. The total amounts of ROS present in cells were measured using an ROS assay kit.

Results: Here, we found that aloin inhibited the proliferation and migration of HGC-27 and BGC-823 gastric cancer cells using a combination of EdU, colony formation, wound healing and transwell assays. Further investigations revealed that aloin decreased the protein expression levels of cyclin D1, N-cadherin, and the matrix metalloproteinases (MMP)-2 and MMP-9; increased E-cadherin expression in a dose-dependent manner; inhibited reactive oxygen species (ROS) generation; and mediated the activation of Akt-mTOR, signal transducer and activator of transcription-3 (Stat3), and NF-κB signalling pathways. Our results also indicated that aloin is able to attenuate the expression levels of the two regulatory proteins of nicotinamide adenine dinucleotide phosphate oxidase 2 (NOX2), $p47^{phox}$ and $p22^{phox}$, but had no effect on the level of $gp91^{phox}$. N-acetylcysteine treatment of gastric cancer cells inhibited ROS production and Akt-mTOR, Stat3, and IκBα phosphorylation. Taken together, our data suggest that aloin inhibits the proliferation and migration of gastric cancer cells by downregulating NOX2–ROS-mediated activation of the Akt-mTOR, Stat3, and NF-κB signalling pathways.

Conclusion: Our findings suggest a potential role for aloin in the prevention of gastric cancer cell proliferation and migration and provide novel insights into the anti-cancer properties of aloin.

Keywords: aloin, gastric cancer, proliferation, migration, nicotinamide adenine dinucleotide phosphate oxidase 2, reactive oxygen species

Introduction

Aloin (ALO) is a bioactive component that is extracted from aloe vera. It has been reported to have anti-inflammatory,[1,2] anti-oxidant,[3] and anti-tumour effects.[4,5] In addition, ALO has been reported to inhibit proliferation and induce the apoptosis of various tumour cells.[1,5,6] However, the molecular mechanism(s) underlying ALO's anti-cancer activity remain to be elucidated.

Correspondence: Zhilin Qi
Department of Biochemistry and Molecular Biology, Wannan Medical College, 22 Wenchang West Road, Wuhu, Anhui 241002, People's Republic of China
Email 422627721@qq.com

submit your manuscript | www.dovepress.com
DovePress
http://doi.org/10.2147/DDDT.S219247

Gastric cancer (GC) is the fourth most common cancer and the second leading cause of cancer deaths worldwide.[7] Despite various therapeutic approaches to improve the survival rate of patients with GC, the effectiveness of the treatments that are currently available remains unsatisfactory.[8] Therefore, there is an urgent requirement to identify novel medicines for the adjuvant treatment of GC. Our previous study showed that ALO could induce GC cell apoptosis by regulating the activation of MAPK signalling pathways.[9] Here, we focused our investigation on the effects of ALO on GC cell proliferation and migration.

Many pro-survival signals affect the proliferation and metastasis of cancer cells. The PI3K/Akt/mTOR signalling pathway plays an important role in the development of malignant tumours by inducing the survival, differentiation and angiogenesis of tumour cells.[10] Akt-mTOR signalling pathway activation leads to the phosphorylation of the ribosomal protein S6 kinase (P70S6K), which in turn regulates the expression of its target genes.[11,12] In addition, the signal transducer and activator of transcription-3 (Stat3) protein is constitutively active in cancer cells. Various upstream kinases such as Janus-activated kinases (JAKs) and Src family kinases induce Stat3 phosphorylation. Activated Stat3 then translocates to the nucleus and regulates the transcription of anti-apoptotic and proliferative genes.[13,14] Several studies have reported that the NF-κB signalling pathway is involved in tumour proliferation and metastasis. For example, bone marrow stromal cell antigen 2 promotes cell proliferation and migration and induces NF-κB activation in GC cells. Pristimerin, a naturally occurring triterpenoid, targets the NF-κB pathway to inhibit the proliferation, migration and invasion of oesophageal squamous cell carcinoma cells.[15,16]

Reactive oxygen species (ROS) have important roles in mediating cell proliferation, migration and angiogenesis through the regulation of many key intracellular signalling pathways including Akt, Stat3, and NF-κB.[17] Nicotinamide adenine dinucleotide phosphate (NADPH) oxidases (NOXs) are an important source of ROS.[18] NOX2, also known as $gp91^{phox}$, is a member of the NOX family that is constitutively associated with $p22^{phox}$ in the plasma membrane. The activation of NOX2 involves its interactions with $p40^{phox}$, $p47^{phox}$, $p67^{phox}$ and the small GTPase Rac1.[19] In our previous study, we found that ALO plays an anti-inflammatory role through its regulation of ROS-mediated JAK/Stat signalling pathway activation in RAW264.7 cells.[2] However, it is not known if ALO prevents GC proliferation and migration through its regulation of ROS-mediated signalling pathways. In this study, our main aim was to investigate if ALO affects GC cell proliferation and migration by targeting NOX2–ROS-mediated pro-survival signalling pathways. Our findings provide novel insights into the anti-cancer effects of ALO on GC cells.

Materials and Methods

Reagents and Antibodies

ALO (purity: 99.8%) was purchased from Selleck Chemicals (Houston, TX, USA). N-acetyl-L-cysteine (NAC) was obtained from Sigma-Aldrich (St. Louis, MO, USA). The Super Lumia ECL HRP substrate kit was purchased from Abbkine Inc (Wuhan, China). The EdU proliferation detection kit was purchased from RiboBio Co., Ltd. (Guangzhou, China). The Cell Counting Kit-8 (CCK-8) was obtained from KeyGen Biotech Co., Ltd. (Nanjing, China). The ROS assay Kit was purchased from the Beyotime Institute of Biotechnology (Haimen,China). Primary antibodies against β-actin, GAPDH, p-Src, p-Stat3, p-Akt, Akt, p-mTOR, mTOR, p-P70S6K, P70S6K, p-S6, S6, p-IκB, and $gp91^{phox}$ were all purchased from Cell Signalling Technology (Beverly, MA, USA). The $p47^{phox}$ and p65 primary antibodies were obtained from Santa Cruz Biotechnology (Dallas, TX, USA). The $p22^{phox}$ primary antibody was purchased from ABclonal Biotechnology Co., Ltd (Hubei, China). Secondary antibodies coupled to the IRDye800 fluorophore for use with the Odyssey Infrared Imaging System were purchased from LI-COR Biosciences (Lincoln, NE, USA).Horseradish peroxidase-conjugated anti-mouse IgG and anti-rabbit IgG secondary antibodies were obtained from Cell Signalling Technology (Beverly, MA, USA).

Cell Culture

GC HGC-27 and BGC-823 cells were purchased from GuangZhou Cellcook Biotech Co., Ltd. (Guangzhou, China). HGC-27 cells were cultured at 37 °C and 5% CO_2 in RPMI-1640 medium (Gibco; Thermo Fisher Scientific, Inc., Waltham, MA, USA) containing 10% non-essential amino acids. BGC-823 cells were cultured in DMEM medium (Gibco), which was supplemented with 10% foetal bovine serum (FBS; Lonsera, South America), 100 μg/mL streptomycin, and 100 U/mL penicillin (Beyotime Institute of Biotechnology, Haimen,China).

CCK-8 Assay

HGC-27 and BGC-823 cells were seeded in 96-well cell culture plates at a density of 1×10^4 and then exposed to a range of doses of ALO for 24 h. For the CCK-8 assay, 10 μL of CCK-8 working solution was added to each well and incubated for another 2 h at 37 °C and 5% CO_2. The absorbance was then measured using a Multiskan™ GO plate reader (Thermo Fisher Scientific, Inc.) at 450 nm. Each treatment was performed in triplicate, and the data are shown as mean ± SD.

Colony Formation Assay

Cells were seeded in 6-well cell culture plates at 200 cells/well and then incubated for 24 h to allow cell attachment. A range of doses of ALO were then added to each well. Following ALO treatment for 24 h, the cell medium was removed and the cells were cultured with new medium for 2 weeks at 37 °C and 5% CO_2. Colonies were fixed in 4% paraformaldehyde for 20 min and then stained with crystal violet for 30 min at room temperature. Colonies were counted under a light microscope: those containing ≥25 cells were classed as a colony.

EdU Assay

Cells were seeded in 24-well plates and cultured for 24 h at 37 °C and 5% CO_2. Once the cells had reached 80% confluency, their proliferation capacity was determined by performing the EdU assay according to the manufacturer's instructions. Briefly, following ALO treatment, cultured cells labelled with EdU were reacted with Apollo® fluorescent dyes, and their nuclei were stained with DAPI. After staining, the cells were observed by fluorescence microscopy (100× magnification; Olympus, Tokyo, Japan).

Cell Cycle Analysis

Cells were seeded in 12-well plates and treated with ALO for 24 h. The cell cycle distribution was then determined using a cell cycle detection kit according to the protocol provided by KeyGen Biotech Co., Ltd. (Nanjing, China). Briefly, cells were collected following trypsinisation, rinsed twice with cold PBS, and fixed with 70% ethanol for 24 h at 4 °C. After washing three times with PBS, RNase A and propidium iodide were added to the wells and incubated at 37 °C for 30 min. Flow cytometry (BD Biosciences, Franklin Lakes, NJ, USA) was then used to detect the cell cycle distribution of the cells. FlowJo 7.6.1 software was used for data analysis.

Wound Healing Assay

Cells were seeded in 12-well plates and cultured to 90%–100% monolayer confluency at 37 °C and 5% CO_2. A straight scratch line was then gently made across the well using a new 200 μL pipette tip, and the detached cells were removed by two gentle PBS washes. The cells were then treated with a range of doses of ALO for 24 h, and then observed using light microscopy (100× magnification; Olympus) at 0 and 24 h. The results were analysed using ImageJ version 1.52 software.

Transwell Assay

Cell migration assays were performed using 24-well cell culture plates with an 8 μm pore membrane (EMD Millipore, Billerica, MA, USA). Briefly, cells were treated with different doses of ALO for 24 h and suspended in DMEM or 1640 medium without FBS. A cell suspension (200 μL) containing 2×10^4 cells was placed in the upper chamber, and 600 μLDMEM or 1640 medium supplemented with 20% FBS was added to the lower chamber. After 24 h incubation at 37 °C and 5% CO_2, cells on the upper surface were wiped away gently, whereas cells that migrated to the lower surface were fixed with 4% paraformaldehyde for 20 min and stained with 0.1% crystal violet diluted in methanol for 30 min at room temperature. Images of the migrated cells were captured using a fluorescence inverted microscope (100× magnification; Olympus).

Western Blotting and Immunoprecipitation

HGC-27 and BGC-823 cells were seeded in 12-well plates and treated with ALO for the times indicated. The medium in each well was then discarded, and the cells were washed with cold PBS. Next, RIPA cell lysis buffer containing protease inhibitors (Beyotime Institute of Biotechnology, Haimen, China) was added to the wells and incubated on ice for 30 min. Lysates were centrifuged (14,300×g) for 10–15 min at 4 °C, and the supernatants were collected. Protein concentrations were measured using a BCA Protein Assay Kit (Beyotime Institute of Biotechnology, Haimen, China). For Western blotting, equivalent amounts of protein (50 μg) from each sample was loaded onto 12% or 10% SDS-PAGE gels and the separated proteins were electroblotted onto nitrocellulose membranes (Pall Corporation, Port Washington, NY, USA). The membranes were then blocked with 5% skimmed milk for 1 h at room temperature, washed with PBS, and probed with primary

antibodies at 4 °C overnight. For visualisation, either an IRDye800 fluorophore-conjugated secondary antibody or a HRP conjugated secondary antibodies were used to probe the membrane (1 h at room temperature) and antigen–antibody complexes were detected by using either a LI-COR Odyssey Infrared Imaging System (LI-COR Biosciences) or a chemiluminescence imaging system (Clinx, Shanghai, China). For immunoprecipitation, proteins were initially incubated with the indicated primary antibody (1:100 dilution) overnight at 4 °C. Next, precleared proteinA/G plus agarose beads were added, and the mixtures were incubated for a further2 h at 4 °C. The beads were then washed four times with cold lysis buffer and resuspended in electrophoresis buffer. These samples were then boiled and analysed by using Western blotting. In addition, aliquots from all cell lysates were analysed to determine the expression levels of related proteins. ImageJ version 1.52 software was used for all densitometry analyses.

ROS Detection and Measurement

The total amounts of ROS present in cells were measured using an ROS assay kit according to the manufacturer's protocol. Briefly, HGC-27 and BGC-823 cells were treated with a range of doses of ALO for 12 h and were then incubated with the fluorescent probe DCFH-DA for 20 min. The cells were subsequently washed three times with serum-free cell culture medium to remove the unbound DCFH-DA from the cells. The cells were then viewed using a fluorescence inverted microscope (100× magnification; Olympus).

Confocal Microscopy

Cells were seeded into small confocal laser dishes. Following treatment of each dish of cells with a range of ALO concentrations (12 h), the cell culture medium was discarded and the cells were fixed with 4% paraformaldehyde, blocked with 3% bovine serum albumin in PBS (1 h at room temperature), and then incubated with p65 primary antibody (at a dilution of 1:100) overnight at 4 °C. The cells were then washed with PBS then incubated with a goat anti-mouse IgG Alexa Fluor® 488 conjugated fluorescent secondary antibody (1:200 dilution) for 1 h at room temperature in the dark. Finally, DAPI was used to stain the cells in the dark for 3 min. Images were captured using a TCS SP8 confocal microscope (630× magnification; Leica Microsystems GmbH, Wetzlar, Germany).

Statistical Analysis

All data were expressed as mean ± SD. SPSS Version 17.0 software (SPSS, Inc., Chicago, IL, USA) was used for statistical analysis. The results were compared using one-way ANOVA, and P values < 0.05 were considered to be statistically significant.

Results

ALO Inhibits GC Cell Proliferation and Colony Formation

We initially used a CCK-8 assay to detect the effect of ALO on the cell viabilities of both HGC-27 and BGC-823 GC cell lines. Following treatment with a range of ALO concentrations, the viabilities of both GC cell lines were suppressed in a dose-dependent manner (Figure 1A). Next, we used an EdU assay to determine the inhibitory effect of ALO on GC cell proliferation. Our results revealed that the amount of EdU-positive cells was clearly reduced after the treatment of both cell lines with ALO. This inhibitory effect was again dose dependent (Figure 1B).We also observed that ALO could inhibit the ability of both HGC-27 and BGC-823 cells to form colonies in a dose-dependent manner (Figure 1C).

ALO Suppresses the Migration of GC Cells

We then used wound healing and transwell assays to determine the effect of ALO on the migration of GC cells. As shown in Figure 2A, the healing rate of scratches clearly decreased following ALO treatment. Transwell assays also showed that ALO treatment was able to reduce the migration of BGC-823 and HGC-27 cells in a dose-dependent manner (Figure 2B).

ALO Decreases cyclin D1 Expression and Causes Cell Cycle Arrest at the S and G2 Phases

To investigate the underlying molecular mechanism for the inhibition of cell proliferation by ALO, we determined the expression levels of cyclin D1 and cyclin E1 and the cell cycle distribution in GC cells treated with ALO. As shown in Figure 3A, we observed a clear reduction in cyclin D1 expression levels in both BGC-823 and HGC-27 cells. In contrast, the expression level of cyclin E1 was unchanged in both cell lines. Cell cycle distribution analysis of control (untreated) BGC-823 cells indicated that 89.16% of the cells were in the G1phase and 9.52% were in the S and G2 phases. However, following treatment of these cells with 100 and 200 μg/mL of ALO, the

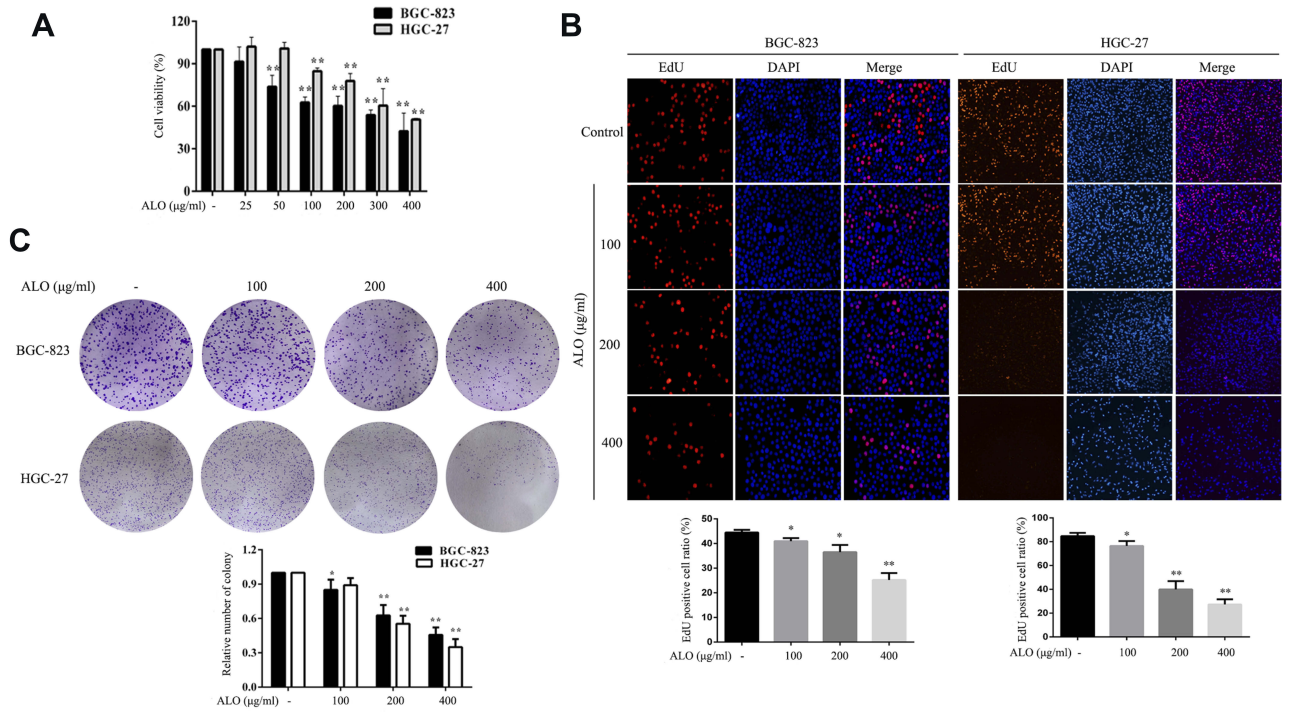

Figure 1 ALO decreases the viability and proliferation of two gastric cancer cell lines. BGC-823 and HGC-27 cells were treated with a range of ALO doses for 24 h. (**A**) Cell viability was determined using a CCK-8 assay. (**B**) The inhibitory effects of ALO on GC proliferation were determined using an EdU assay and (**C**) a colony formation assay. Each experiment was performed in triplicate. Data were expressed as means ± SD, *P < 0.05 and **P < 0.01 vs the control group.

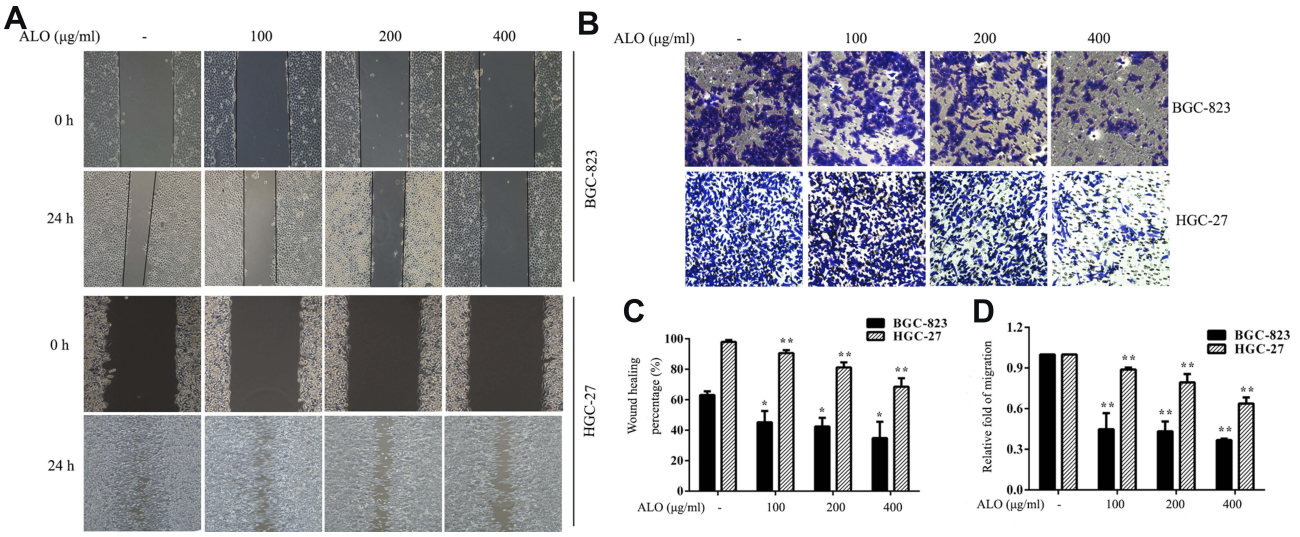

Figure 2 ALO represses the migration of gastric cancer cells. (**A**) A wound healing assay and (**B**) a transwell assay were performed on BGC-823 and HGC-27 cells following ALO treatment for 24 h. (**C, D**) Quantitative analysis of data obtained in the above experiments. Data are presented as means ± SD of three independent experiments. *P < 0.05 and **P < 0.01 vs the control group.

percentage of cells in the G1 phase decreased to 70.17% and 44.6%, respectively, whereas the percentage of S and G2 phase cells increased to 23.42% and 34.17%, respectively. Cell cycle distribution analysis of control (untreated) HGC-27 cells indicated that 56.08% of the cells were in the G1phase and 31.88% were in the S and G2 phases. Following cell treatment with 100 and 200 μg/mL of ALO, the percentage of G1 phase cells decreased to 35.55% and 33.98%, respectively; however, the percentage of S and G2 phase cells increased to 61.08% and 61.38%, respectively (Figure 3B). These results suggested that ALO treatment of GC cells caused cell cycle arrest at the S and G2 phases.

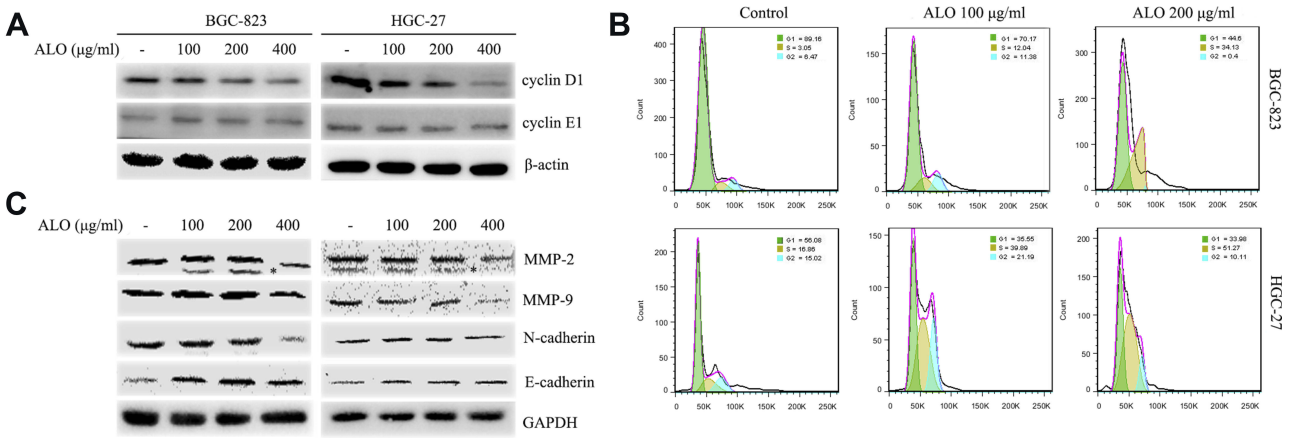

Figure 3 ALO attenuates cyclin D1, MMPs and EMT marker expression levels and causes cell cycle arrest of gastric cancer cells. Following ALO treatment for 24 h, the protein expression levels of (**A**) cyclin D1 and E1. (**C**) MMP-2, MMP-9, N-cadherin and E-cadherin were determined in gastric cancer cells using Western blotting. β-actin or GAPDH was used as a loading control. * nonspecific bands. (**B**) Cell cycle distributions were determined after ALO treatment using flow cytometry.

ALO Inhibits the Expression of MMPs and EMT Marker Proteins

Metalloproteinases (MMPs) and the epithelial–mesenchymal transition (EMT) are thought to be involved in the migration and invasion of tumour cells.[20,21] Therefore, we investigated the effects of ALO on the expression of MMPs and EMT marker proteins. As shown in Figure 3C, ALO clearly reduced the expression levels of MMP-2 and MMP-9. Furthermore, the expression level of N-cadherin (a mesenchymal marker) was observed to decrease, whereas the expression of E-cadherin (an epithelial marker) increased following treatment of both BGC-823 and HGC-27 cell lines with ALO. However, the observed changes in EMT marker expression levels in HGC-27 cells were considered non-significant.

ALO Suppresses Activation of the Akt-mTOR, Stat3, and NF-κB Signalling Pathways

To investigate the signalling pathways involved in the ALO-mediated inhibition of GC cells, the phosphorylation levels of Akt, Stat3, and IκBα were determined by Western blotting. As shown in Figure 4A, ALO treatment attenuated phosphorylation and activation of the Akt/mTOR/P70S6K signalling pathway, in a dose-dependent manner. The phosphorylation, and therefore the activation of Src, Stat3, and IκBα was also suppressed by ALO treatment (Figure 4B). Additionally, we tracked the nuclear translocation of p65 using a confocal microscopy assay. In control (untreated) GC cells, p65 was clearly observed in nuclei; however, the p65 nuclear level was clearly reduced following ALO treatment (Figure 5). Taken together, these results suggested that ALO is able to inhibit GC proliferation and migration by preventing the activation of the Akt, Stat3, and NF-κB signalling pathways.

ALO Decreases ROS Production in GC Cells

ROS play a vital role during cancer initiation and progression, and high ROS levels in cancer cells can be exploited for the specific targeting of cancer cells.[22,23] We investigated the effect of ALO treatment on ROS generation in GC cells. ALO was able to markedly reduce the production of ROS in both cell lines compared with their untreated (control) counterparts (Figure 6A).

ALO Suppresses $P22^{phox}$ and $P47^{phox}$ Expression Levels

NOXs are one of the major source of endogenous ROS generation in response to various stimuli.[24] Moreover, NOX2-dependent ROS generation is involved in the proliferation and invasion of cancer cells.[25] Therefore, we also examined the effect of ALO on NOX2 expression in BGC-823 and HGC-27 cell lines. Although ALO had no detectable effect on $gp91^{phox}$ expression, it markedly reduced the expression levels of both $p22^{phox}$ and $p47^{phox}$in both of the cell lines (Figure 6B).

ROS Accumulation Causes the Activation of Akt, Stat3, and IκBα Signalling Pathways in GC Cells

An increase in intracellular ROS levels activates tumorigenesis-associated pathways including the MAPK, NF-κB, and Akt pathways.[26,27] To examine

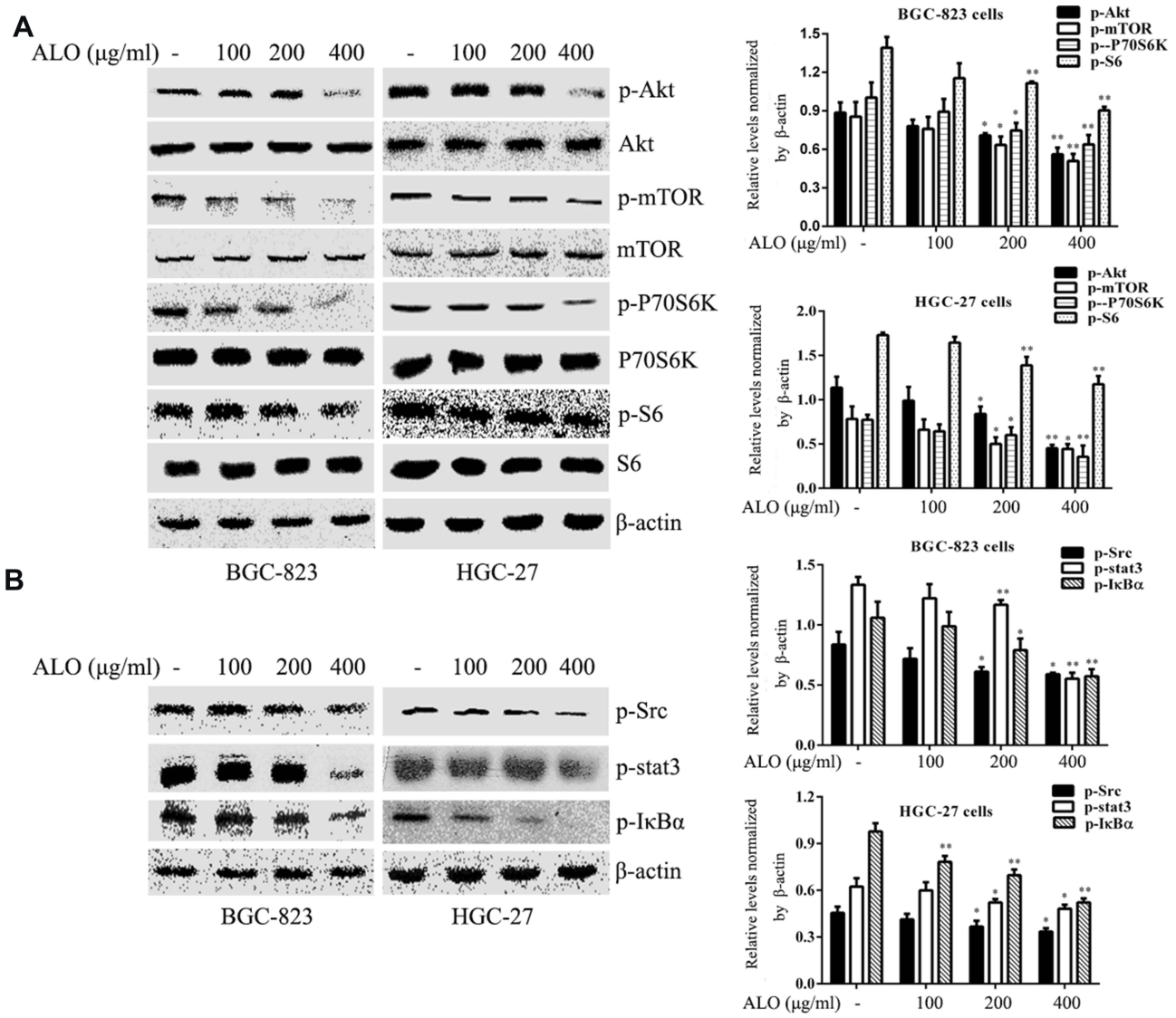

Figure 4 ALO inhibits activation of the Akt/mTOR, Stat3, and NF-κB signalling pathways in gastric cancer cells. BGC-823 and HGC-27 cells were treated with ALO for 12 h. (**A**) the phosphorylation levels and the total amounts of Akt, mTOR, P70S6K and S6 proteins were determined using Western blotting. (**B**) The phosphorylation levels of Src, Stat3, and IκBα were also determined by Western blotting. All protein levels were normalised relative to β-actin. Data are presented as means ± SD of three independent experiments. *P < 0.05 and **P < 0.01 vs the control group.

whether ROS are the upstream activators of Akt, NF-κB, and Stat3 pathways in GC cells, we treated cells with the anti-oxidant NAC. NAC not only blocked intracellular ROS accumulation but also suppressed the activation of Akt-mTOR, Stat3, and IκBα in GC cells (Figure 7).

Discussion

Our previous study revealed that ALO induced the apoptosis of GC cells.[9,28] Here, we investigated if ALO was able to inhibit GC proliferation and migration and then elucidated the underlying molecular mechanisms of its action. Our results suggest that ALO is able to inhibit both the proliferation and migration of GC cells by regulating the activation of NOX2–ROS-mediated pro-survival signal pathways.

The inhibition of tumour cell proliferation is a fundamental strategy to halt tumour progression. We found that ALO demonstrably decreased the viability of two GC cell lines,BGC-823 and HGC-27, in a dose-dependent manner. On the basis of these findings, a range of suitable ALO doses (100, 200, and 400 μg/mL) were used in subsequent experiments to determine the inhibitory effects of ALO on GC cell proliferation and

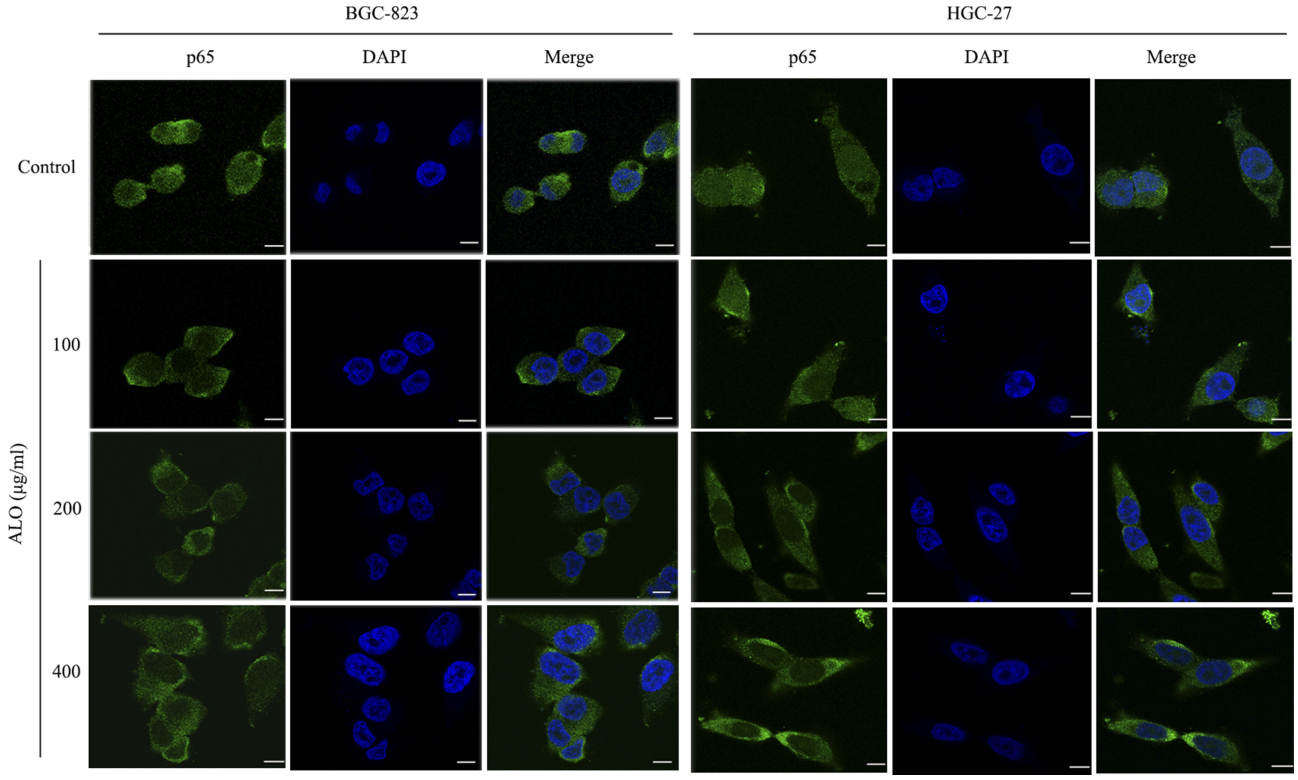

Figure 5 ALO suppresses the nuclear translocation of p65. Following treatment with ALO for 12 h, the location of p65 in the nucleus and cytoplasm of gastric cancer cells was determined by using a confocal microscopy assay. Nuclei were stained with DAPI (blue), and p65 is shown in red. Scale bar: 25 μm.

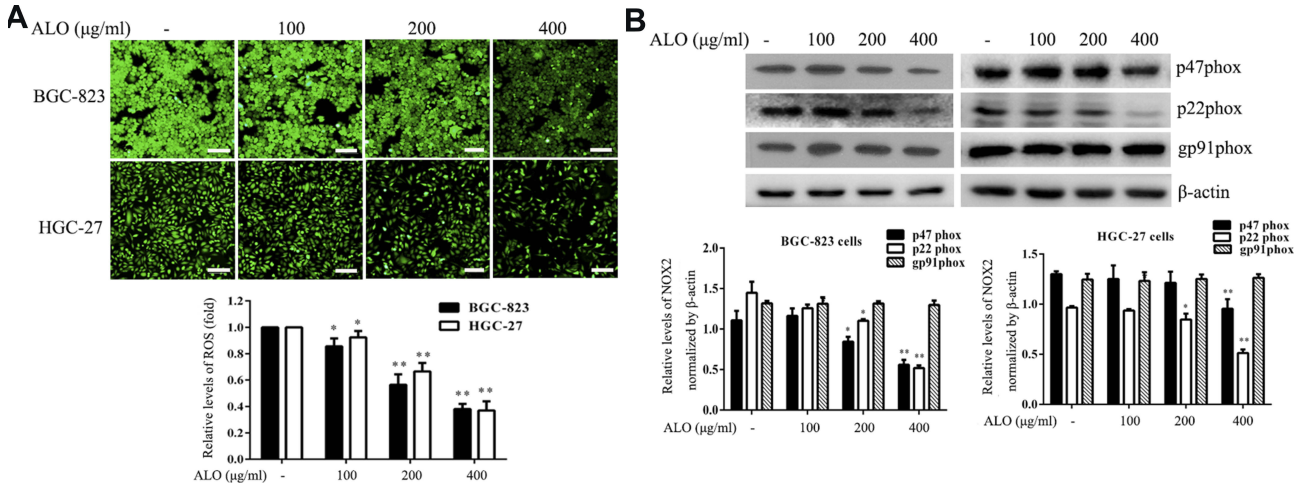

Figure 6 ALO attenuates ROS generation and NOX2 expression. Gastric cancer cells were treated with a range of doses of ALO for 12 h. (**A**) ROS production was then determined using a detection kit. (**B**) Following ALO treatment, total protein was collected, and the protein expression levels of $p47^{phox}$, $p22^{phox}$ and $gp91^{phox}$ were determined using Western blotting. Each experiment was performed in triplicate. Data are shown as means ± SD. *P < 0.05 and **P < 0.01 vs the control group.

migration. Our results revealed that ALO treatment significantly suppressed colony formation and proliferative abilities of GC cells compared with control (untreated) cells (Figure 1). Both our wound healing and transwell assays showed that the migration capacity of GC cells was also blocked by ALO in a dose-dependent manner (Figure 2). To explore these inhibitory activities in more detail, we determined the expression levels of cyclin, MMPs, and EMT marker proteins and investigated cell cycle distribution in control (untreated) GC cells and those treated with ALO. As shown in Figure 3, ALO treatment decreased the expression levels of cyclin D1, MMP-2 and MMP-9. Furthermore, particularly in BGC-823 cells, the expression levels of E-cadherin were found

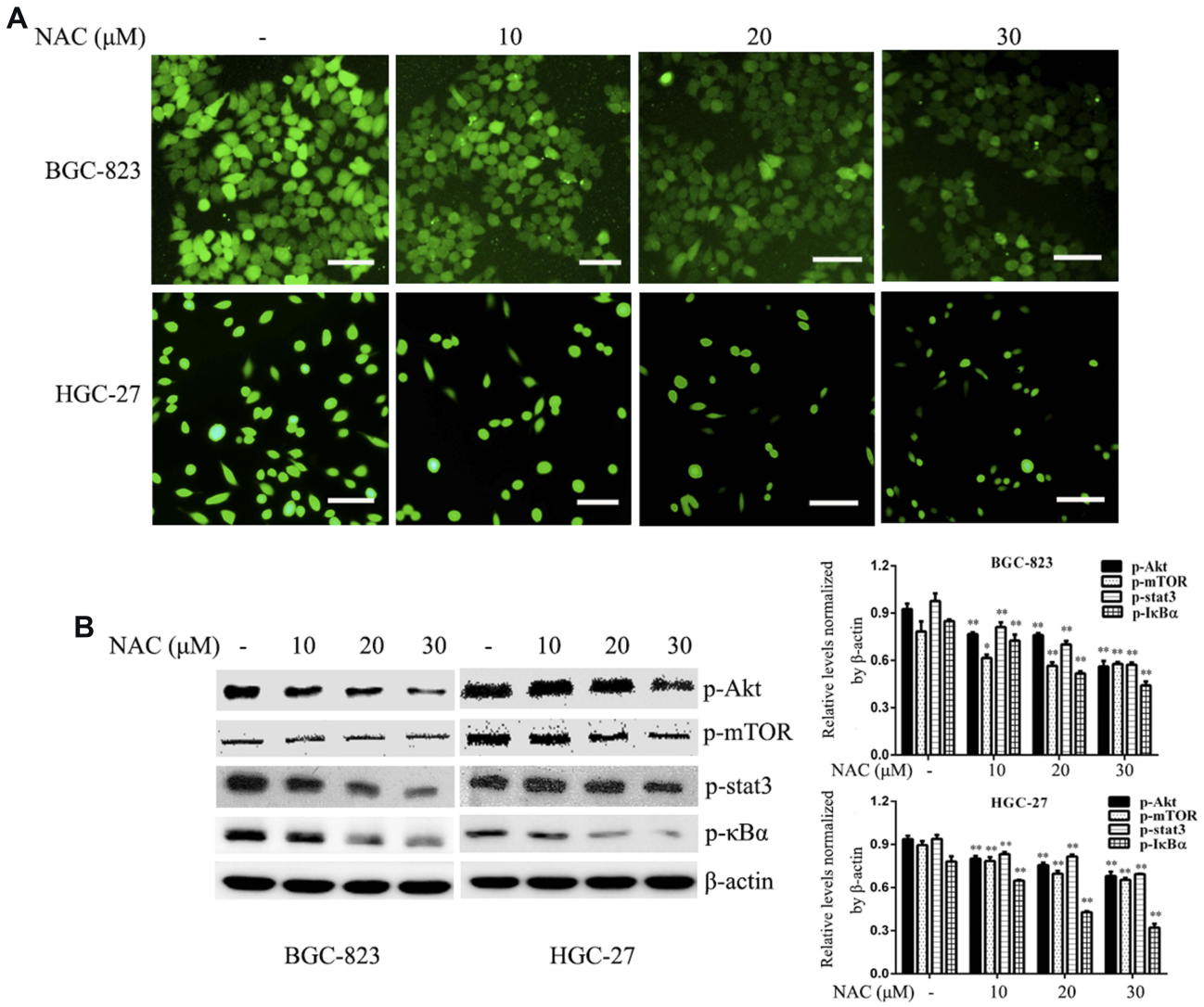

Figure 7 ROS markedly inhibits ROS generation and mediates the activation of pro-survival signalling pathways. Gastric cancer cells were treated with different doses of NAC for 12 h. (**A**) ROS production was determined using an ROS detection kit. (**B**) The phosphorylation levels of Akt, mTOR, Stat3, and IκBα were determined by Western blotting. β-actin was used as a loading control. Each experiment was performed in triplicate. Data are shown as means ± SD, *P < 0.05 and **P < 0.01 vs the control group.

to increase, whereas N-cadherin expression levels decreased following ALO treatment. The observed differences in ALO efficacy on EMT marker expression in the two cell lines tested are likely to be a cell-specific effect. In addition, GC cells treated with ALO were arrested at the S and G2 phases.

Akt/mTOR, Stat3, and NF-κB signalling pathways play an important role in cell proliferation and migration.[29–31] ALO treatment caused a marked decrease in the activation of the Akt/mTOR/P70S6K and Stat3 signalling pathways. Furthermore, IκBα phosphorylation was also considerably reduced (Figure 4).

The NF-κB heterodimers p65 and p50 are sequestered in the cytosol of unstimulated cells through their binding to IκB. However, IκB phosphorylation leads to its degradation, and the free p50 and p65 then translocate to the nucleus where they activate NF-κB-dependent gene transcription.[31] Therefore, we tracked the nuclear translocation of p65 upon ALO treatment of GC cells. As shown in Figure 5, p65 nuclear levels were found to significantly decrease following ALO treatment. Taken together, our results suggest that ALO inhibits GC cell proliferation and migration by suppressing the activation of Akt/mTOR, Stat3, and NF-κB signalling pathways.

Increasing evidence indicates a role for ROS-associated signalling in the proliferation, survival and other phenotypic behaviours of cancer cells.[32] In this study, we observed a marked decrease in ROS generation

in GC cells following ALO treatment (Figure 6A) This suggested that ALO attenuates GC cell proliferation and migration by suppressing ROS production. The inhibition of ROS production has been reported to prevent the metastasis of cancer cells.[33] In addition, increasing evidence has revealed that the augmentation of ROS production is beneficial for the migration of tumours.[34,35] Other studies have found that ROS use multiple mechanisms to affect the initiation, growth, and spread of cancer and may promote or suppress cancer development,[36] suggesting they act as a "double-edged sword." As NOX2 is a known source of ROS production, we investigated the effect of ALO treatment on NOX2 expression in GC cells. Our results revealed that ALO caused a significant decrease in the expression levels of $p47^{phox}$ and $p22^{phox}$ but had no effect on $gp91^{phox}$ expression (Figure 6). NOX2 activation requires its interaction with $p40^{phox}$, $p47^{phox}$, $p67^{phox}$ and the small GTPase Rac1.[19] The $p47^{phox}$ regulatory subunit and the catalytic, membrane-bound subunit $gp91^{phox}$ play critical roles in the activation of NADPH oxidases. Upon cell activation, the cytosolic $p47^{phox}$ migrates to the plasma membrane, where it associates with $gp91^{phox}$ to activate NADPH oxidases.[37,38] Our IP experiment indicated that the binding of $gp91^{phox}$ and $p47^{phox}$ in GC cells was inhibited by ALO treatment (Figure S1).These results suggest that ALO could attenuate ROS generation by downregulating NOX2 activation. To determine if ROS are upstream targets of intracellular pro-survival signalling pathways, we investigated the effects of NAC treatment on GC cells. NAC is a ROS scavenger, which removes intracellular ROS. We found that NAC treatment reduced ROS production and suppressed the phosphorylation of Akt/mTOR, Stat3, and IκBα signalling pathways (Figure 7). These data suggested that ROS could mediate the activation of pro-survival signalling pathways.

In conclusion, the results of this study suggest that ALO inhibits GC cell proliferation and migration by downregulating NOX2–ROS-mediated activation of the Akt/mTOR, Stat3, and NF-κB signalling pathways, providing novel insights into its anti-tumour activities.

Acknowledgments

This work was supported by Natural Science Foundation of China (grant no. 81601380; 81872371), Natural Science Research Project of Anhui Colleges and Universities (grant no. KJ2016SD59); Outstanding Young Talent Support Key Projects of Anhui Colleges and Universities (grant no. gxyqZD2016173), Active Biological Macromolecules Research Provincial Key Laboratory Project (grant no. 1306C083008), National college Students' innovation and Entrepreneurship training project (grant nos. 201810368024 and 201710368002) and the Anhui Province College Students' Innovation and Entrepreneurship Training project (grant no. 201710368166 and 201810368103).

Disclosure

The authors report no conflicts of interest in this work.

References

1. Luo X, Zhang H, Wei X, et al. Aloin suppresses lipopolysaccharide-induced inflammatory response and apoptosis by inhibiting the activation of NF-kappaB. *Molecules*. 2018;23(3):517. doi:10.3390/molecules23030517
2. Ma Y, Tang T, Sheng L, et al. Aloin suppresses lipopolysaccharideinduced inflammation by inhibiting JAK1STAT1/3 activation and ROS production in RAW264.7 cells. *Int J Mol Med*. 2018;42 (4):1925–1934. doi:10.3892/ijmm.2018.3796
3. Liu FW, Liu FC, Wang YR, et al. Aloin protects skin fibroblasts from heat stress-induced oxidative stress damage by regulating the oxidative defense system. *PLoS ONE*. 2015;10(12):e0143528. doi:10.1371/journal.pone.0143528
4. Esmat AY, Said MM, Khalil SA. Aloin: a natural antitumor anthraquinone glycoside with iron chelating and non-atherogenic activities. *Pharm Biol*. 2015;53(1):138–146. doi:10.3109/13880209.2014.912239
5. Wan L, Zhang L, Fan K, et al. Aloin promotes A549 cell apoptosis via the reactive oxygen speciesmitogen activated protein kinase signaling pathway and p53 phosphorylation. *Mol Med Rep*. 2017;16 (5):5759–5768. doi:10.3892/mmr.2017.7379
6. Buenz EJ. Aloin induces apoptosis in Jurkat cells. *Toxicol in Vitro*. 2008;22(2):422–429. doi:10.1016/j.tiv.2007.10.013
7. Wang L, Chen X, Du Z, et al. Curcumin suppresses gastric tumor cell growth via ROS-mediated DNA polymerase gamma depletion disrupting cellular bioenergetics. *J Exp Clin Cancer Res*. 2017;36(1):47. doi:10.1186/s13046-017-0513-5
8. An JX, Ma MH, Zhang CD, et al. miR-1236-3p inhibits invasion and metastasis in gastric cancer by targeting MTA2. *Cancer Cell Int*. 2018;18:66. doi:10.1186/s12935-018-0560-9
9. Wang Z, Tao H, Ma Y, et al. Aloin induces apoptosis via regulating the activation of MAPKs signaling pathway in human gastric cancer cells in vitro. *Nan Fang Yi Ke Da Xue Xue Bao*. 2018;38 (9):1025–1031. doi:10.12122/j.issn.1673-4254.2018.09.01
10. Han C, Xing G, Zhang M, et al. Wogonoside inhibits cell growth and induces mitochondrial-mediated autophagy-related apoptosis in human colon cancer cells through the PI3K/AKT/mTOR/p70S6K signaling pathway. *Oncol Lett*. 2018;15(4):4463–4470. doi:10.3892/ol.2018.7852
11. Steelman LS, Chappell WH, Abrams SL, et al. Roles of the Raf/MEK/ERK and PI3K/PTEN/Akt/mTOR pathways in controlling growth and sensitivity to therapy-implications for cancer and aging. *Aging (Albany NY)*. 2011;3(3):192–222. doi:10.18632/aging.v3i3
12. Ataie-Kachoie P, Pourgholami MH, Bahrami-B F, et al. Minocycline attenuates hypoxia-inducible factor-1α expression correlated with modulation of p53 and AKT/mTOR/p70S6K/4E-BP1 pathway in ovarian cancer in vitro and in vivo studies. *Am J Cancer Res*. 2015;5(2):575–588.
13. Kim DH, Park KW, Chae IG, et al. Carnosic acid inhibits STAT3 signaling and induces apoptosis through generation of ROS in human colon cancer HCT116 cells. *Mol Carcinog*. 2016;55(6):1096–1110. doi:10.1002/mc.22353

14. Lin L, Liu A, Peng Z, et al. STAT3 is necessary for proliferation and survival in colon cancer-initiating cells. *Cancer Res*. 2011;71(23):7226–7237. doi:10.1158/0008-5472.CAN-10-4660
15. Tu Y, Tan F, Zhou J, et al. Pristimerin targeting NF-kappaB pathway inhibits proliferation, migration, and invasion in esophageal squamous cell carcinoma cells. *Cell Biochem Funct*. 2018;36(4):228–240. doi:10.1002/cbf.3335
16. Liu W, Cao Y, Guan Y, et al. BST2 promotes cell proliferation, migration and induces NF-kappaB activation in gastric cancer. *Biotechnol Lett*. 2018;40(7):1015–1027. doi:10.1007/s10529-018-2562-z
17. Qi S, Kou X, Lv J, et al. Ampelopsin induces apoptosis in HepG2 human hepatoma cell line through extrinsic and intrinsic pathways: involvement of P38 and ERK. *Environ Toxicol Pharmacol*. 2015;40(3):847–854. doi:10.1016/j.etap.2015.09.015
18. Kim SY, Jeong JM, Kim SJ, et al. Pro-inflammatory hepatic macrophages generate ROS through NADPH oxidase 2 via endocytosis of monomeric TLR4-MD2 complex. *Nat Commun*. 2017;8(1):2247. doi:10.1038/s41467-017-02325-2
19. Xu C, Wang X, Gu C, et al. Celastrol ameliorates Cd-induced neuronal apoptosis by targeting NOX2-derived ROS-dependent PP5-JNK signaling pathway. *J Neurochem*. 2017;141(1):48–62. doi:10.1111/jnc.2017.141.issue-1
20. Sun C, Wang Z, Zheng Q, et al. Salidroside inhibits migration and invasion of human fibrosarcoma HT1080 cells. *Phytomedicine*. 2012;19(3–4):355–363. doi:10.1016/j.phymed.2011.09.070
21. Ablin RJ, Owen S, Jiang WG. Prostate transglutaminase (TGase-4) induces epithelial-to-mesenchymal transition in prostate cancer cells. *Anticancer Res*. 2017;37(2):481–487. doi:10.21873/anticanres
22. Wang C, Wang Z, Liu W, et al. ROS-generating oxidase NOX1 promotes the self-renewal activity of CD133+ thyroid cancer cells through activation of the Akt signaling. *Cancer Lett*. 2019;447:154–163. doi:10.1016/j.canlet.2019.01.028
23. Nogueira V, Hay N. Molecular pathways: reactive oxygen species homeostasis in cancer cells and implications for cancer therapy. *Clin Cancer Res*. 2013;19(16):4309–4314. doi:10.1158/1078-0432.CCR-12-1424
24. Guo Y, Han B, Luo K, et al. NOX2-ROS-HIF-1alpha signaling is critical for the inhibitory effect of oleanolic acid on rectal cancer cell proliferation. *Biomed Pharmacother*. 2017;85:733–739. doi:10.1016/j.biopha.2016.11.091
25. Liu L, Rezvani HR, Back JH, et al. Inhibition of p38 MAPK signaling augments skin tumorigenesis via NOX2 driven ROS generation. *PLoS ONE*. 2014;9(5):e97245. doi:10.1371/journal.pone.0097245
26. Cao L, Chen X, Xiao X, et al. Resveratrol inhibits hyperglycemia-driven ROS-induced invasion and migration of pancreatic cancer cells via suppression of the ERK and p38 MAPK signaling pathways. *Int J Oncol*. 2016;49(2):735–743. doi:10.3892/ijo.2016.3559
27. Liu L, Yang Z, Xu Y, et al. Inhibition of oxidative stress-elicited AKT activation facilitates PPARgamma agonist-mediated inhibition of stem cell character and tumor growth of liver cancer cells. *PLoS ONE*. 2013;8(8):e73038. doi:10.1371/journal.pone.0073038
28. Tao H, Tang T, Wang S, et al. The molecular mechanisms of Aloin induce gastric cancer cells apoptosis by targeting high mobility group box 1. *Drug Des Devel Ther*. 2019;13:1221–1231. doi:10.2147/DDDT.S201818
29. Hossan MS, Chan ZY, Collins HM, et al. Cardiac glycoside cerberin exerts anticancer activity through PI3K/AKT/mTOR signal transduction inhibition. *Cancer Letter*. 2019;453:57–73. doi:10.1016/j.canlet.2019.03.034
30. Sun Y, Liu L, Wang Y, et al. Curcumin inhibits the proliferation and invasion of MG-63 cells through inactivation of the p-JAK2/p-STAT3 pathway. *Onco Targets Ther*. 2019;12:2011–2021. doi:10.2147/OTT.S172909
31. El-Ashmawy NE, El-Zamarany EA, Khedr EG, et al. Activation of EMT in colorectal cancer by MTDH/NF-kappaB p65 pathway. *Mol Cell Biochem*. 2019;457(1–2):83–91. doi:10.1007/s11010-019-03514-x
32. Saikolappan S, Kumar B, Shishodia G, et al. Reactive oxygen species and cancer: a complex interaction. *Cancer Lett*. 2019;452:132–143. doi:10.1016/j.canlet.2019.03.020
33. Schexnayder C, Broussard K, Onuaguluchi D, et al. Metformin inhibits migration and invasion by suppressing ROS production and COX2 expression in MDA-MB-231 breast cancer cells. *Int J Mol Sci*. 2018;19(11):3612. doi:10.3390/ijms19113692
34. Kim U, Kim CY, Lee JM, et al. Phloretin inhibits the human prostate cancer cells through the generation of reactive oxygen species. *Pathol Oncol Res*. 2019. doi:10.1007/s12253-019-00643-y
35. Li Q, Zhang Y, Jiang Q. MFAP5 suppression inhibits migration/invasion, regulates cell cycle and induces apoptosis via promoting ROS production in cervical cancer. *Biochem Biophys Res Commun*. 2018;507(1–4):51–58. doi:10.1016/j.bbrc.2018.10.146
36. Martner A. Aydin E and Hellstrand K. NOX2 in autoimmunity, tumor growth and metastasis. *J Pathol*. 2019;247(2):151–154. doi:10.1002/path.5175
37. Sumimoto H, Miyano K and Takeya R. Molecular composition and regulation of the Nox family NAD(P)H oxidases. *Biochem Biophys Res Commun*. 2005;338(1):677–686. doi:10.1016/j.bbrc.2005.08.210
38. Li J, Fan L, Christie MR, Shah A. Acute tumor necrosis factor alpha signaling via NADPH oxidase in microvascular endothelial cells: role of p47phox phosphorylation and binding to TRAF4. *Mol Cell Biol*. 2005;25(6):2320–2330. doi:10.1128/MCB.25.6.2320-2330.2005